Calorimetric study of single-crystal $CsFe_2As_2$

A. F. Wang,[1] B. Y. Pan,[2] X. G. Luo,[1] F. Chen,[1] Y. J. Yan,[1] J. J. Ying,[1] G. J. Ye,[1] P. Cheng,[1]
X. C. Hong,[2] S. Y. Li,[2] and X. H. Chen[1,*]

[1]*Hefei National Laboratory for Physical Science at Microscale and Department of Physics, University of Science and Technology of China, Hefei, Anhui 230026, People's Republic of China*

[2]*Department of Physics, State Key Laboratory of Surface Physics, and Laboratory of Advanced Materials, Fudan University, Shanghai 200433, People's Republic of China*

(Received 24 February 2013; revised manuscript received 25 April 2013; published 13 June 2013)

We measured the resistivity and the specific heat of $CsFe_2As_2$ single crystals, which were grown by using a self-flux method. The $CsFe_2As_2$ crystal shows a sharp superconducting transition at 1.8 K with a transition width of 0.1 K. The sharp superconducting transition and pronounced jump in specific heat indicate high quality of the crystals. A large $\Delta C_p/T_c$ accompanying a very low T_c, nonexponential dependence of the lowest temperature $\Delta C_p/T$ and an $H^{1/2}$ dependence of $\Delta\gamma(H)$ are observed in the superconducting-state specific heat. Combined with the fitting results by the α model for the superconducting-state specific heat, a pairing symmetry with nodal gaps was suggested in $CsFe_2As_2$.

DOI: 10.1103/PhysRevB.87.214509 PACS number(s): 74.70.Xa, 74.25.Bt, 74.25.F−, 74.20.Rp

I. INTRODUCTION

The discovery of iron-based superconductors has opened a new window for unveiling the physics of high-temperature superconductivity besides cuprates.[1–3] Among the various families of iron-based superconductors discovered till now, AFe_2As_2 (A = alkali earth, alkali, and Eu, the so-called 122 system), which has the $ThCr_2Si_2$ structure, is the most investigated family due to the easy growth of sizable high-quality single crystals.[4] In this 122 system, KFe_2As_2, as the end member of the $Ba_{1-x}K_xFe_2As_2$ series, shows some unique properties. Firstly, superconductivity with $T_c \sim 4$ K can be realized in KFe_2As_2 without purposely doping. Secondly, a very clean single crystal with residual resistivity ratio (RRR) exceeding 1000 can be quite easily achieved, which is a good start point to study intrinsic physical properties. It was proposed that interband interaction that links the hole and electron Fermi surfaces (FS) produces an $s_\pm$ pairing symmetry in most of the iron-based superconductors. However, angle-resolved photoemission spectroscopy (ARPES) and the de Haas-van Alphen (dHvA) experiments revealed that the electron pockets disappeared and the large hole sheets centered around the Γ point dominate FS in KFe_2As_2.[5,6] Therefore the pairing interaction could be distinct from other iron-based superconductors. The nodes on superconducting gaps have been detected by thermal conductivity,[7,8] penetration depth,[9] and NMR.[10,11] The measurements of thermal conductivity,[8,12] specific heat,[13] and penetration depth[9] support a d-wave superconducting state in KFe_2As_2. In contrast, recent ultrahigh-resolution laser ARPES suggested a nodal s-wave superconductor with highly unusual FS-selective multi-gap structure.[14] Whether those nodes are accidental or imposed by symmetry still remains an open question. As a consequence, further investigation on analogous compounds would be significant to clarify the underlying physics in the AFe_2As_2 system. In the present article, we will report the crystal growth and characterization of the analogous compound $CsFe_2As_2$.

Superconductivity at 2.6 K was observed in the polycrystalline $CsFe_2As_2$ sample.[15] But few physical properties have been reported so far because high-quality single crystals are not available until now. The difficulty of growing sizable $CsFe_2As_2$ single crystals mainly lies in the extremely high chemical activity and low melting point of Cs. In the present article, we have successfully overcome this problem by using the stainless steel sample container assembly,[16] which can be sealed in the glove box (O_2 content is less than 1 ppm) mechanically. As a result, sizable high-quality single crystals of $CsFe_2As_2$ were grown. The $CsFe_2As_2$ single crystals were characterized by x-ray diffraction (XRD), resistivity, magnetic susceptibility, and specific heat. The sharp superconducting transition temperature and obvious specific jump indicate good quality of the single crystals. We observed a large $\Delta C_p/T_c$ accompanied by a very low T_c, nonexponential dependence of the lowest temperature $\Delta C_p/T$, and an $H^{1/2}$ dependence of $\Delta\gamma(H)$ in the superconducting-state specific heat of $CsFe_2As_2$. Based on these observations and the fitting results with the α model for the superconducting-state specific heat, a pairing symmetry with nodal gaps was suggested.

II. EXPERIMENTAL DETAILS

High-quality $CsFe_2As_2$ single crystals are grown by the self-flux technique. The Cs chunks, Fe and As powders were weighted according to the ratio of Cs:Fe:As = 6:1:6. Typically, 1.5 grams of the mixture of Fe and As powders were loaded into a 10-mm diameter alumina crucible, and freshly cut Cs pieces were placed on top of the mixture. Then the alumina crucible with a lid was sealed in a stainless steel container assembly. The whole preparation process was carried out in a glove box in which high pure argon atmosphere was filled (O_2 content is less than 1 ppm). Considering the low melting point of Cs (T_m = 28 °C), the room temperature must be kept below 20 °C. The sealed stainless steel assembly was then sealed inside an evacuated quartz tube. The quartz tube was placed in a box furnace and slowly heated up to 200 °C. It was kept at 200 °C for 400 minutes, which allows full reaction of Cs and the mixture. Then the sample was heated up to 950 °C in 10 hours. The temperature was kept still for 10 hours and then slowly cooled to 550 °C at a rate of 3 °C/h. After cooling down to

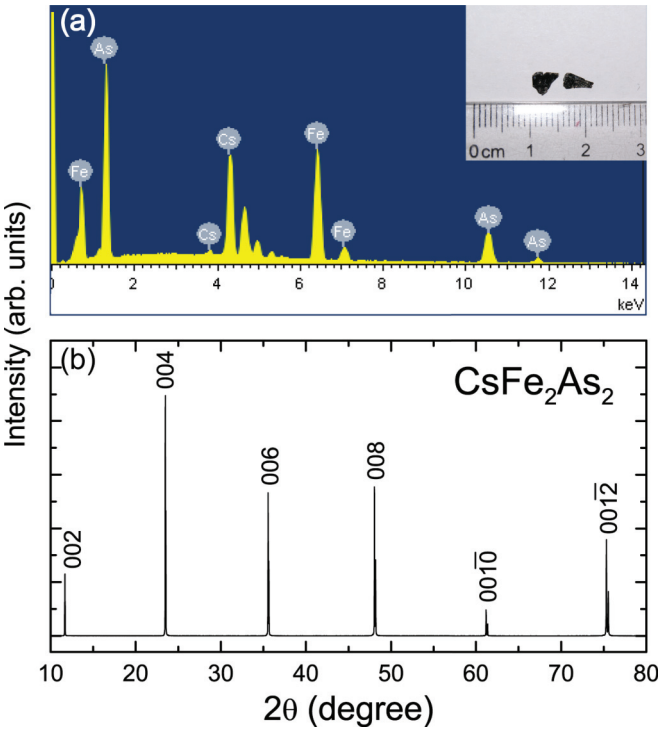

FIG. 1. (Color online) (a) A typical EDX spectrum for a $CsFe_2As_2$ single crystal, the inset shows a photograph of the $CsFe_2As_2$ single crystal together with a millimeter scale. (b) X-ray diffraction pattern of the $CsFe_2As_2$ single crystal.

room temperature by switching off the furnace, shiny platelike crystals can be easily picked up from the alumina crucible. The single crystals are stable in air or alcohol for several days.

XRD was performed on a SmartLab-9 diffracmeter(Rikagu) from 10° to 80° with a scanning rate of 4° per minute. The actual chemical composition of the single crystal is determined by energy dispersive x-ray spectroscopy (EDX) mounted on the field emission scanning electronic microscope (FESEM), Sirion 200. The magnetic susceptibility was measured using a vibrating sample magnetometer (VSM) (Quantum Design). The direct current (dc) resistivity was measured by the conventional four-probe method using the PPMS-9T (Quantum Design). Resistivity and specific heat down to 50 mK were measured in a dilution refrigerator on PPMS.

III. RESULTS

The typical size of as-grown single crystals is about 5 mm × 3 mm × 0.03 mm, as shown in the inset of Fig. 1(a). Elemental analysis was performed using EDX. A typical EDX spectrum is shown in Fig. 1(a), and the obtained atomic ratio of Cs:Fe:As is roughly 20.76: 40.52: 38.71. The atomic ratio is consistent with the composition $CsFe_2As_2$ within instrumental error. Figure 1(b) shows the single crystal XRD pattern for $CsFe_2As_2$. Only (00*l*) reflections can be recognized, indicating that the crystal is well orientated along the *c* axis. The *c*-axis lattice parameter was estimated to be $c = 15.13$ Å, consistent with a previous report on the polycrystalline samples.[15]

Figure 2 shows the in-plane resistivity as a function of the temperature for a $CsFe_2As_2$ single crystal. The resistivity exhibits metallic behavior in the entire temperature range between 1.9 K to 300 K. The behavior of the resistivity resembles that of the counterpart compound KFe_2As_2. The resistivity begins to drop rapidly at 1.88 K and reaches zero at 1.8 K. The superconducting transition temperature T_c in the following text is defined as the temperature when the resistivity reaches zero. The sharp superconducting transition with a transition width less than 0.1 K indicates high quality of the crystal. The T_c of $CsFe_2As_2$ is slightly lower than that reported on the polycrystalline sample.[15] Residual resistivity $\rho_0 = 1.8\ \mu\Omega$ is obtained by fitting the data with the formula $\rho = \rho_0 + AT^{1.5}$.[17] The residual resistivity ratio (RRR) $\rho(300K)/\rho_0$ is estimated to be 200, comparable with those of KFe_2As_2 grown with FeAs flux,[7,18] but much smaller than those in crystals of KFe_2As_2 grown with KAs.[12,16]

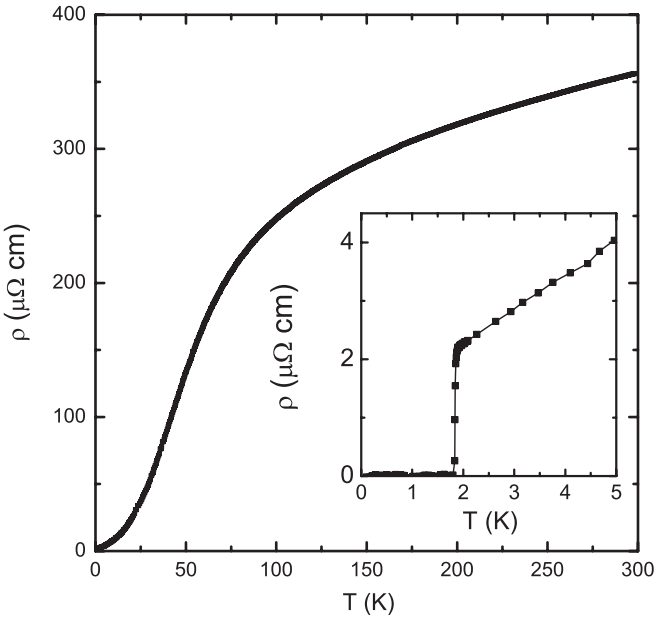

FIG. 2. Resistivity plotted as a function of temperature for a $CsFe_2As_2$ single crystal. The inset is the zoom plot of resistivity around the superconducting transition.

Figure 3 shows the temperature dependence of the in-plane magnetic susceptibility for a $CsFe_2As_2$ single crystal under

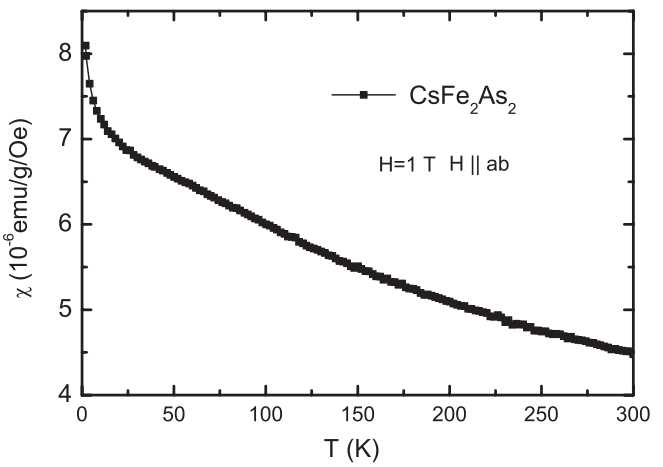

FIG. 3. Temperature dependence of the magnetic susceptibility of the $CsFe_2As_2$ single crystal collected at $H = 1$ T with $H \parallel ab$.

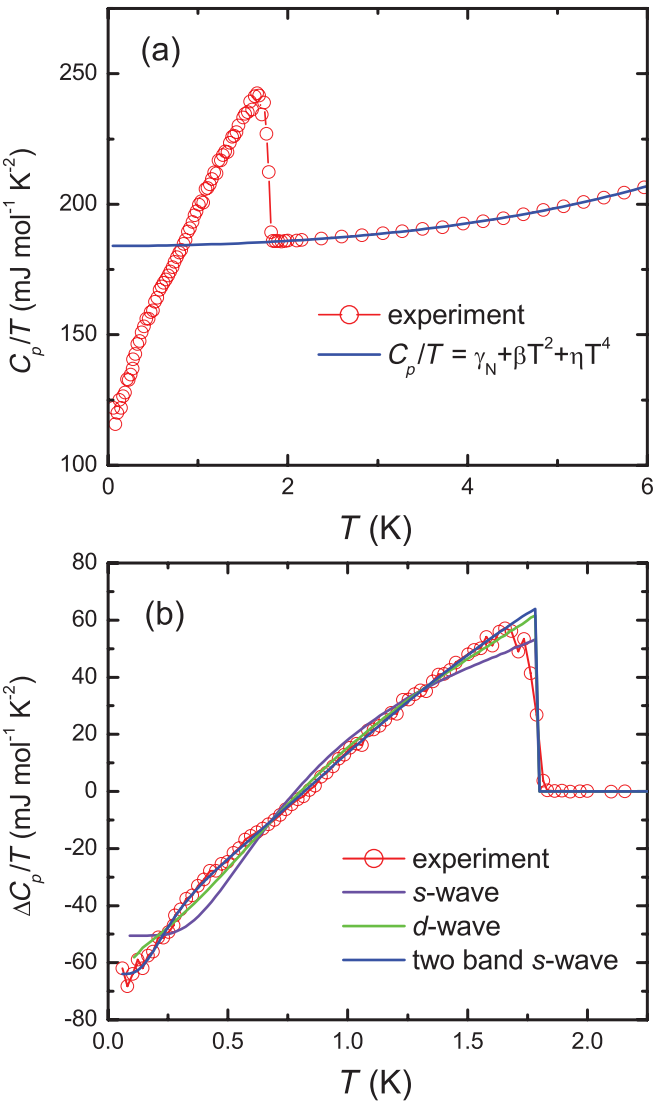

FIG. 4. (a) Temperature dependence of specific heat divided by temperature for $CsFe_2As_2$, $C_p(T)/T$. The blue solid line is the fitting for the data between 1.9 and 10 K (data below 6 K are shown). The fitting function is described in the text. (b) Temperature dependence of the difference in the electronic specific heat between the superconducting and the normal states. The violet, green, and blue solid lines represent fits for the experimental data by using single-band s-wave ($\alpha = 1.42$), single-band d-wave ($\alpha = 1.93$), and two-band s-wave α ($\alpha_1 = 1.21$, $\alpha_2 = 3.33$) models, respectively.

$H = 1$ T in the normal state. The $CsFe_2As_2$ single crystal shows paramagnetic behavior from 300 to 2 K. No magnetic anomaly corresponding to cluster glass as reported in KFe_2As_2 was observed here.[19]

In Fig. 4(a), we show the temperature dependence of the specific heat of $CsFe_2As_2$ down to 50 mK under zero magnetic field. A pronounced jump due to the superconducting transition is observed below 1.8 K, consistent with the resistivity measurement. This indicates the high quality of the present crystals. The normal-state specific heat can be well fitted by $C_{\text{normal}}(T) = \gamma_N T + C_{\text{lattice}}(T)$, where $\gamma_N T$ and $C_{\text{lattice}}(T) = \beta T^3 + \eta T^5$ are electron and phonon contributions, respectively.[20] The solid line in Fig. 4(a) is the best fit to the C_p/T above T_c (1.9 to 10 K). We obtained $\gamma_N = 184.01$ mJ mol^{-1} K^{-2}, $\beta = 0.466$ mJ mol^{-1}K^{-4}, and $\eta = 0.00474$ mJ mol^{-1} K^{-6}. From this value of β and by using the formula $\Theta_D = [12\pi^4 k_B N_A Z/(5\beta)]^{1/3}$, where N_A is the Avogadro constant and Z is the total number of atoms in one unit cell, the Debye temperature (Θ_D) is estimated to be 275 K. This value is comparable to that of KFe_2As_2,[21] $Ba_{0.68}K_{0.32}Fe_2As_2$,[23] and $LaFeAsO_{0.9}F_{0.1-\delta}$.[22] It should be pointed out that $\gamma_N = 184.01$ mJ mol^{-1} K^{-2} is very large. The γ_N reported on $Ba_{0.68}K_{0.32}Fe_2As_2$, $Ba(Fe_{0.925}Co_{0.075})_2As_2$, and $FeTe_{0.57}Se_{0.43}$ is 50, 23.8, and 26.6 mJ mol^{-1} K^{-2}, respectively.[23–25] The specific heat jump is only about 35% of γ_N, which is similar to the case of KFe_2As_2.[10,13,19,21] The normal-state specific heat can be calculated by

$$\gamma_N = \frac{1}{3}\pi^2 k_B^2 N(E_F)(1+\lambda),$$

where $N(E_F)$ is the density of states (DOS) at the Fermi surface and λ reflects the coupling strength. The large γ_N indicates the existence of moderately large electron correlations in $CsFe_2As_2$. In Ref. 26, the large γ_N in KFe_2As_2 is attributed to proximity to an orbitally selective Mott transition due to strong Hund correlation. Terashima *et al.* interpreted the large γ_N in KFe_2As_2 by considering the very large effective masses of electrons ranging from 6–18m_e (m_e the free electron mass) observed in de Haas-van Alphen measurements.[6] γ_N of KFe_2As_2 is calculated to be 84 mJ mol^{-1} K^{-2} from the effective masses of electrons obtained by ARPES measurements,[27] consistent with the de Haas-van Alphen and specific heat measurement. ARPES measurements on our crystal of $CsFe_2As_2$ also revealed the existence of abnormally large density of states or effective masses of electrons, which may be useful to understand the very large γ_N here.[28]

Estimating the value of $\Delta C_p/\gamma_N T_c$ is a traditional method to estimate the coupling strength of a superconductor, with larger values implying stronger coupling. $\Delta C_p/\gamma_N T_c$ in $CsFe_2As_2$ can be estimated to be about 0.35, and similar values about 0.35 and 0.4 were reported on KFe_2As_2 with RRR of 67 and 650.[10,29] This value is much smaller than that (=1.43) expected for weak-coupling BCS superconductors, which could be attributed to weak coupling strength or a non-BCS superconductivity in $CsFe_2As_2$. In addition, $\Delta C_p/T_c$ at $T_c = 1.8$ K is estimated to be about 64 mJ mol^{-1} K^{-2}. The specific heat jump was observed to be about 120, 30, and 56 mJ mol^{-1} K^{-2} in $Ba_{0.68}K_{0.32}Fe_2As_2$, $Ba(Fe_{0.925}Co_{0.075})_2As_2$, and $FeTe_{0.57}Se_{0.43}$, which have T_c of 14–40 K.[23–25] Considering the low T_c of $CsFe_2As_2$, the jump is quite large and has a value about 350 times larger than that calculated from $\Delta C_p/T_c = aT_c^2$ ($a \sim 0.056$ mJ mol^{-1} K^{-4}), the scaling behavior proposed by Bud'ko, Ni, and Canfield (BNC).[30] In KFe_2As_2, $\Delta C_p/T_c \approx 67$ mJ mol^{-1} K^{-2} with $T_c = 3.4$ K,[21,31] which also lies far above the BNC trend. Since most iron-based superconductors obey the phenomenological law of BNC, this suggests that the pairing symmetry in $CsFe_2As_2$ could be similar to that in KFe_2As_2, but different from that of other iron-based superconductors.

In Fig. 4(a), a large residual superconducting electronic specific heat can be observed in the $T \to 0$ limit. γ_{res} can be estimated to be about 108.1 mJ mol^{-1} K^{-2} from Fig. 4(a).

Though finite values of γ_{res} are a common feature in the specific measurements of the iron-based superconductors,[23,24] our γ_{res} is extraordinarily large. Large γ_{res} was commonly observed in KFe_2As_2.[10,13,31] with one exception that $\gamma_{res} \simeq 0$ was reported in KFe_2As_2 with RRR = 650.[29] The large γ_{res} observed in KFe_2As_2 was thought to arise from a nonsuperconducting fraction by some authors.[29,31,32] The magnetic contribution from a cluster glass was also thought to be a possible reason of such large γ_{res} in KFe_2As_2.[13,33] It should be noted that $CsFe_2As_2$ and KFe_2As_2 here have very low residual resistivity in the $T \to 0$ limit and very high γ_{res}, while in other pnictide superconductors, such as $Ba(Fe_{1-x}Co_x)_2As_2$,[24] the residual resistivity in the $T \to 0$ limit is relatively high but very small γ_{res} can be observed. These facts suggest that the large γ_{res} in $CsFe_2As_2$ (as well as in KFe_2As_2) can not be simply ascribed to some nonsuperconducting impurity, because the low residual resistivity in the $T \to 0$ limit and the quite high RRR indicate a low impurity level. Furthermore, a cluster glass origin can be ruled out for interpreting the large γ_{res} since no feature for cluster glass can be observed in the magnetic susceptibility in Fig. 3. Considering the large ratio of γ_{res} proportional to γ_N observed in KFe_2As_2 and LaOFeP,[34] which were thought to be nodal superconductors, the large γ_{res} and large γ_{res}/γ_N ratio observed in $CsFe_2As_2$ might be a sign of a nodal superconductor.

Figure 4(b) shows the superconducting electronic specific heat difference between the superconducting and normal states, $\Delta C_p(T) = C_p(T) - C_{normal}(T) = C_{es} - \gamma_N T$, where $C_{es} = C_p(T) - C_{lattice}(T)$ is the superconducting electronic specific heat. The entropy conservation is confirmed to be satisfied. We tried to fit the data using the "α model:"[35]

$$\Delta C_p = C_{es}/T - \gamma_0 = \frac{4N_F}{k_B T^3}\int_0^{\infty}\int_0^{2\pi} \frac{e^{\xi/k_B T}}{(1+e^{\xi/k_B T})^2} \times \left[\varepsilon^2 + \Delta^2(\theta,T) - \frac{T}{2}\frac{d\Delta^2(\theta,T)}{dT}\right] d\theta d\varepsilon - \gamma_0,$$

where γ_0 is a fitting constant. The fitting results are shown in Fig. 4(b). The best fit by a single-band BCS α model yields the reduced gap value $\alpha(= \Delta/k_B T) = 1.42$. It indicates that $\Delta C_p/T$ can not be described by a single-band BCS α model. As a consequence, our results exclude the single-band s-wave pairing symmetry. Then, single-band d-wave and two-band s-wave models were used, as shown in Fig. 4(b).[20,36] The two-band s-wave model seems to give rise to a better fitting quality, with the two gaps of $\alpha_1 = 1.21$ and $\alpha_2 = 3.33$, which seems consistent with a weakly coupled two-band superconductor with one gap larger than the BCS gap ($\alpha = 1.76$) and one smaller.[36] The fitting in the single-band d-wave model has a subtle weak quality with $\alpha = 1.93$. The possibility of d-wave cannot be excluded, according to the discussions above.

In the low-temperature limit, the s-wave model predicts $\Delta C/T \propto T^{-5/2}\exp(-\Delta/k_B T)$, while in the clean d-wave model, $C_{es} \sim T^2$, which gives $\Delta C_p/T \propto T$, as have been observed in the organic superconductors κ-(BEDT-TTF)$_2$Cu[N(CN)$_2$]Br and κ-(BEDT-TTF)$_2$Cu(NCS)$_2$.[37] The low-temperature part of the specific heat in Fig. 4(b) roughly follows a linear temperature dependence rather than an exponential one, therefore, the gap symmetry seems most likely to be d wave. The thermal conductivity measured on the same batch of $CsFe_2As_2$ single crystals indicates nodal superconducting gap symmetry.[17] It has been reported that there is an anomaly around 0.7 K in C_p/T of KFe_2As_2, which was thought to be related to the impurity or disordered magnetism contribution in the sample,[19,29,33] and higher quality of crystals can almost eliminate such an anomaly in KFe_2As_2.[13] But the anomaly was also attributed to small superconducting gaps on parts of the Fermi surface by some authors.[38] Such a very weak anomaly may slightly affect the result of the fit. This may make it a little ambiguous to deduce the pairing symmetry just from the fittings, since the main difference between the fitting in d-wave and two-band s-wave models lies below 0.55 K (although the difference is very weak). Therefore we measured the temperature dependence of specific heat under different magnetic fields to investigate the field dependence of the Sommerfeld coefficient $\gamma(H)$ since the field dependence of $\gamma(H)$ can provide information for the superconducting pairing symmetry.

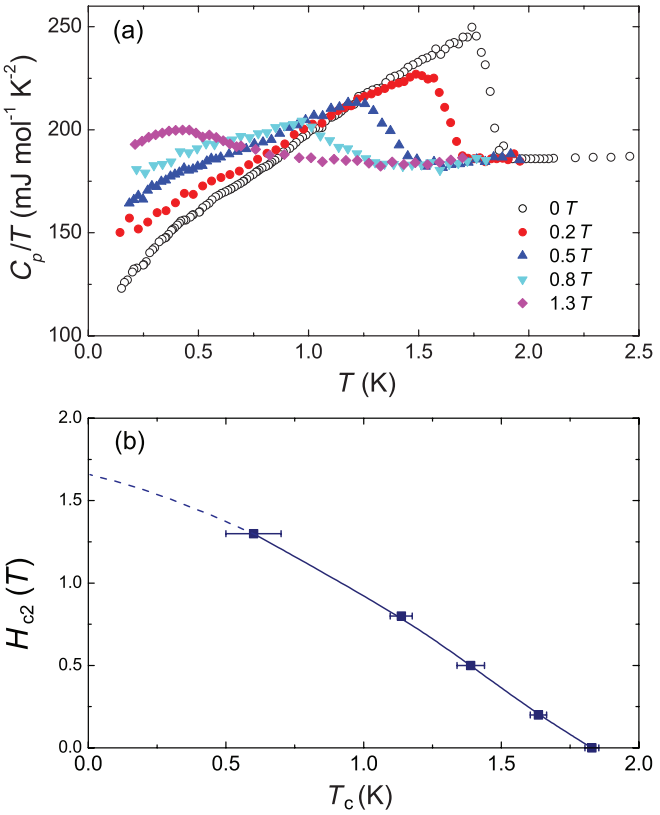

FIG. 5. (Color online) (a) Temperature dependence of C_p/T under various magnetic fields. (b) The upper critical field H_{c2} determined by the specific heat shown in (a). The dashed line guides one's eye to estimate $H_{c2}(0)$.

The C_p/T taken under various magnetic fields is shown in Fig. 5(a). With increasing external field, the superconductivity is gradually suppressed and the electronic contribution is enhanced. $T_c(H)$ can be determined by the midpoint over the superconducting jump in specific heat. We plotted $T_c(H)$ with the magnetic field in Fig. 5(b). The upper critical field at $T = 0$ limit $H_{c2}(0)$ can be estimated to be about 1.65 T, which is nearly the same as that obtained from transport measurements.[17]

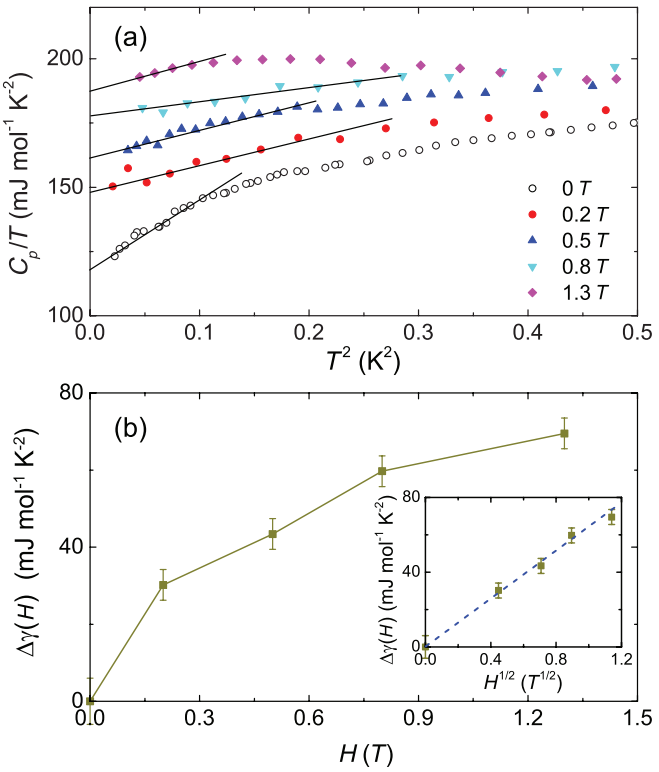

FIG. 6. (Color online) (a) Low-temperature C_p/T plotted as a function of T^2 under various magnetic fields. The solid lines are linear fittings for the lowest-temperature range. (b) Field dependence of $\Delta\gamma(H) = \gamma(H) - \gamma_{\rm res}$. The inset shows the plot of $\Delta\gamma(H)$ vs $H^{1/2}$, where the dashed line shows the linear fitting.

We then plotted the C_p/T taken under various magnetic fields against T^2 in Fig. 6(a), from which we can determine the Sommerfeld coefficient under different magnetic fields [$\gamma(H)$]. For a full gapped superconductor, the quasiparticle excitations are confined inside the vortex cores, and as a consequence $\gamma(H)$ mainly arises from the density of states of such localized quasiparticles, which would lead to $\gamma(H) \propto H$.[39] However, as the superconducting gap possesses a deep minimum or a node, delocalized quasiparticles would exist and they could lead to a nonlinear magnetic field dependence, such as the relation of $\gamma(H) \propto H^{1/2}$ observed in cuprate superconductors with d-wave superconducting pairing symmetry. Theoretically, by using a Doppler-shift approach, Volovik showed that for superconductors with line nodes the extended quasiparticle excitations outside the vortex cores would cause a nonlinear magnetic field dependence of the spatially averaged residual density of states $N(\omega = 0, H) \propto N_0\sqrt{H/H_{c2}}$, a result known as the Volovik effect.[40] By fitting the lowest-temperature part of C_p/T linear to T^2, as shown in Fig. 6(a) by the solid lines, $\gamma(H)$ can be determined. We plotted $\Delta\gamma(H) = \gamma(H) - \gamma_{\rm res}$ against H in Fig. 6(b). One can find that $\Delta\gamma(H)$ is far from the linear dependence on H. Therefore isotropic s-wave pairing symmetry can be ruled out. We then plotted $\Delta\gamma(H)$ against $H^{1/2}$, as shown in inset of Fig. 6(b). A linear dependence is observed, that is, $\Delta\gamma(H) \propto H^{1/2}$. This relation $\gamma(H) \propto H^{1/2}$ is similar to the Volovik effect for nodal superconductors. Although we still cannot definitely determine the pairing symmetry of $CsFe_2As_2$, the Volovik-like field dependence of $\gamma(H)$ must exclude an isotropic full gap and favor the existence of nodes in at least some Fermi surfaces; combined with the large $\Delta C_p/T_c$ versus very low T_c, the nonexponential dependence of the lowest temperature $\Delta C_p/T$, the fitting of zero-magnetic-field $\Delta C_p/T$ in Fig. 4(b), the $H^{1/2}$ dependence of $\Delta\gamma(H)$, and the result of thermal conductivity in our previous paper (where the finite κ_0/T in zero field and the field dependence of κ_0/T supported a nodal superconducting gap in $CsFe_2As_2$), we conclude that d wave might be the most possible symmetry for the superconducting pairing. Further measurements, such as ARPES and NMR, should be performed to illustrate the pairing symmetry, similar to the case of KFe_2As_2.

IV. SUMMARY AND CONCLUSIONS

We have successfully grown $CsFe_2As_2$ single crystals using the assembly of a stainless steel container. The sharp drop in resistivity and pronounced jump in specific heat with T_c around 1.8 K indicate the high quality of crystals. The behavior of resistivity, magnetic susceptibility, and specific data resemble the counterpart compound KFe_2As_2. The very large $\Delta C_p/T_c$ at very low T_c, the nonexponential dependence of the lowest temperature $\Delta C_p/T$, the fitting results of zero-magnetic-field $\Delta C_p/T$ in Fig. 4(b), and the $H^{1/2}$ dependence of $\Delta\gamma(H)$ might suggest a pairing symmetry with nodal gaps in $CsFe_2As_2$. More work is required to yield the exact pairing symmetry in this system.

ACKNOWLEDGMENTS

This work is supported by the National Natural Science Foundation of China (Grant NoS. 11190021, 11174266, 51021091), the "Strategic Priority Research Program (B)" of the Chinese Academy of Sciences (Grant No. XDB04040100), the National Basic Research Program of China (973 Program, Grant NoS. 2012CB922002 and 2011CBA00101), and the Chinese Academy of Sciences.

*Corresponding author: chenxh@ustc.edu.cn

[1] Y. Kamihara, T. Watanabe, M. Hirano, and H. Hosono, J. Am. Chem. Soc. **130**, 3296 (2008).
[2] X. H. Chen, T. Wu, G. Wu, R. H. Liu, H. Chen, and D. F. Fang, Nature (London) **453**, 761 (2008).
[3] M. Rotter, M. Tegel, and D. Johrendt, Phys. Rev. Lett. **101**, 107006 (2008).
[4] X. F. Wang, T. Wu, G. Wu, H. Chen, Y. L. Xie, J. J. Ying, Y. J. Yan, R. H. Liu, and X. H. Chen, Phys. Rev. Lett. **102**, 117005 (2009).
[5] T. Sato, K. Nakayama, Y. Sekiba, P. Richard, Y. M. Xu, S. Souma, T. Takahashi, G. F. Chen, J. L. Luo, N. L. Wang, and H. Ding, Phys. Rev. Lett. **103**, 047002 (2009).
[6] T. Terashima, M. Kimata, N. Kurita, H. Satsukawa, A. Harada, K. Hazama, M. Imai, A. Sato, K. Kihou, C. H. Lee, H. Kito,

H. Eisaki, A. Iyo, T. Saito, H. Fukazawa, Y. Kohori, H. Harima, and S. Uji, J. Phys. Soc. Jpn. **79**, 053702 (2010).
[7]J. K. Dong, S. Y. Zhou, T. Y. Guan, H. Zhang, Y. F. Dai, X. Qiu, X. F. Wang, Y. He, X. H. Chen, and S. Y. Li, Phys. Rev. Lett. **104**, 087005 (2010).
[8]J.-Ph. Reid, M. A. Tanatar, A. Juneau-Fecteau, R. T. Gordon, S. René de Cotret, N. Doiron-Leyraud, T. Saito, H. Fukazawa, Y. Kohori, K. Kihou, C. H. Lee, A. Iyo, H. Eisaki, R. Prozorov, and Louis Taillefer, Phys. Rev. Lett. **109**, 087001 (2012).
[9]K. Hashimoto, A. Serafin, S. Tonegawa, R. Katsumata, R. Okazaki, T. Saito, H. Fukazawa, Y. Kohori, K. Kihou, C. H. Lee, A. Iyo, H. Eisaki, H. Ikeda, Y. Matsuda, A. Carrington, and T. Shibauchi, Phys. Rev. B **82**, 014526 (2010).
[10]H. Fukazawa, Y. Yamada, K. Konda, T. Saito, Y. Kohori, K. Kuga, Y. Matsumoto, S. Nakatsuji, H. Kito, P. M. Shirage, K. Kihou, N. Takeshita, C. H. Lee, A. Iyo, and H. Eisaki, J. Phys. Soc. Jpn. **78**, 083712 (2009).
[11]S. W. Zhang, L. Ma, Y. D. Hou, J. Zhang, T. L. Xia, G. F. Chen, J. P. Hu, G. M. Luke, and W. Yu, Phys. Rev. B **81**, 012503 (2010).
[12]A. F. Wang, S. Y. Zhou, X. G. Luo, X. C. Hong, Y. J. Yan, J. J. Ying, P. Cheng, G. J. Ye, Z. J. Xiang, S. Y. Li, and X. H. Chen, arXiv:1206.2030.
[13]M. Abdel-Hafiez, V. Grinenko, S. Aswartham, I. Morozov, M. Roslova, O. Vakaliuk, S. L. Drechsler, S. Johnston, D. V. Efremov, J. Van den Brink, H. Rosner, M. Kumar, C. Hess, S. Wurmehl, A. U. B. Wolter, B. Büchner, E. L. Green, J. Wosnitza, P. Vogt, A. Reifenberger, C. Enss, and R. Klingeler, arXiv:1301.5257.
[14]K. Okazaki, Y. Ota, Y. Kotani, W. Malaeb, Y. Ishida, T. Shimojima, T. Kiss, S. Watanabe, C.-T. Chen, K. Kihou, C. H. Lee, A. Iyo, H. Eisaki, T. Saito, H. Fukazawa, Y. Kohori, K. Hashimoto, T. Shibauchi, Y. Matsuda, H. Ikeda, H. Miyahara, R. Arita, A. Chainani, and S. Shin, Science **337**, 1314 (2012).
[15]Kalyan Sasmal, Bing Lv, Bernd Lorenz, Arnold M. Guloy, Feng Chen, Yu-Yi Xue, and Ching-Wu Chu, Phys. Rev. Lett. **101**, 107007 (2008).
[16]Kunihiro Kihou, Taku Saito, Shigeyuki Ishida, Masamichi Nakajima, Yasuhide Tomioka, Hideto Fukazawa, Yoh Kohori, Toshimitsu Ito, Shin-ichi Uchida, Akira Iyo, Chul-Ho Lee, and Hiroshi Eisaki, J. Phys. Soc. Jpn. **79**, 124713 (2010).
[17]X. C. Hong, X. L. Li, B. Y. Pan, L. P. He, A. F. Wang, X. G. Luo, X. H. Chen, and S. Y. Li, Phys. Rev. B **87**, 144502 (2013).
[18]Taichi Terashima, Motoi Kimata, Hidetaka Satsukawa, Atsushi Harada, Kaori Hazama, Shinya Uji, Hisatomo Harima, Gen-Fu Chen, Jian-Lin Luo, and Nan-Lin Wang, J. Phys. Soc. Jpn. **78**, 063702 (2009).
[19]V. Grinenko, S. L. Drechsler, M. Abdel-Hafiez, S. Aswartham, A. U. B. Wolter, S. Wurmehl, C. Hess, K. Nenkov, G. Fuchs, D. V. Efremov, B. Holzapfel, J. van den Brink, and Buchner, Phys. Status Solidi B **250**, 593 (2012).
[20]A. F. Wang, X. G. Luo, Y. J. Yan, J. J. Ying, Z. J. Xiang, G. J. Ye, P. Cheng, Z. Y. Li, W. J. Hu, and X. H. Chen, Phys. Rev. B **85**, 224521 (2012).
[21]Sergey L. Bud'ko, Yong Liu, Thomas A. Lograsso, and Paul C. Canfield, Phys. Rev. B **86**, 224514 (2012).
[22]G. Mu, X. Y. Zhu, L. Fang, L. Shan, C. Ren, and H. H. Wen, Chin. Phys. Lett. **25**, 2221 (2008).
[23]P. Popovich, A. V. Boris, O. V. Dolgov, A. A. Golubov, D. L. Sun, C. T. Lin, R. K. Kremer, and B. Keimer, Phys. Rev. Lett. **105**, 027003 (2010).
[24]F. Hardy, T. Wolf, R. A. Fisher, R. Eder, P. Schweiss, P. Adelmann, H. v. Löhneysen, and C. Meingast, Phys. Rev. B **81**, 060501(R) (2010).
[25]J. Hu, T. J. Liu, B. Qian, A. Rotaru, L. Spinu, and Z. Q. Mao, Phys. Rev. B **83**, 134521 (2011).
[26]F. Hardy, A. E. Böhmer, D. Aoki, P. Burger, T. Wolf, P. Schweiss, R. Heid, P. Adelmann, Y. X. Yao, G. Kotliar, J. Schmalian, and C. Meingast, arXiv:1302.1696.
[27]T. Yoshida, S. Ideta, I. Nishi, A. Fujimori, M. Yi, R. G. Moore, S. K. Mo, D.-H. Lu, Z. X. Shen, Z. Hussain, K. Kihou, P. M. Shirage, H. Kito, C. H. Lee, A. Iyo, H. Eisaki, and H. Harima, arXiv:1205.6911.
[28]Z. Sun *et al.* (unpublished).
[29]J. S. Kim, E. G. Kim, G. R. Stewart, X. H. Chen, and X. F. Wang, Phys. Rev. B **83**, 172502 (2011).
[30]S. L. Bud'ko, N. Ni, and P. C. Canfield, Phys. Rev. B **79**, 220516(R) (2009).
[31]M. Abdel-Hafiez, S. Aswartham, S. Wurmehl, V. Grinenko, C. Hess, S.-L. Drechsler, S. Johnston, A. U. B. Wolter, B. Büchner, H. Rosner, and L. Boeri, Phys. Rev. B **85**, 134533 (2012).
[32]G. R. Stewart, Rev. Mod. Phys. **83**, 1589 (2011).
[33]V. Grinenko, M. Abdel-Hafiez, S. Aswartham, A. U. B. Wolter-Griaud, C. Hess, M. Kumar, S. Wurmehl, K. Nenkov, G. Fuchs, B. Holzapfel, S.-L. Drechsler, and B. Büchner, arXiv:1203.1585.
[34]S. Suzuki, S. Miyasaka, S. Tajima, T. Kida, and M. Hagiwara, J. Phys. Soc. Jpn. **78**, 114712 (2009).
[35]H. Padamsee, J. Low Temp. Phys. **12**, 387 (1973).
[36]V. Z. Kresin and S. A. Wolf, Physica C **169**, 476 (1990).
[37]O. J. Taylor, A. Carrington, and J. A. Schlueter, Phys. Rev. Lett. **99**, 057001 (2007).
[38]P. Burger, F. Hardy, D. Aoki, A. E. Böhmer, R. Heid, T. Wolf, P. Schweiss, R. Fromknecht, M. J. Jackson, C. Paulsen, and C. Meingast, arXiv:1303.6822.
[39]C. Caroli, P. G. de Gennes, and J. Matricon, Phys. Lett. **9**, 307 (1964).
[40]G. E. Volovik, JETP Lett. **58**, 469 (1993).